Separation Science and Technology
Publication details, including instructions for authors and subscription information:
http://www.informaworld.com/smpp/title~content=t713708471

Effects of Operating Modes on the Rejection Behavior using Ceramic Membranes

T. Y. Chiu[a]; F. J. Garcia-Garcia[b]; A. E. James[c]
[a] School of Applied Sciences, Centre for Water Science, Cranfield University, Bedfordshire, United Kingdom [b] Corrosion and Protection Centre, School of Materials, The University of Manchester, Manchester, United Kingdom [c] School of Chemical Engineering and Analytical Science, The University of Manchester, Manchester, United Kingdom

To cite this Article Chiu, T. Y. , Garcia-Garcia, F. J. and James, A. E.(2008) 'Effects of Operating Modes on the Rejection Behavior using Ceramic Membranes', Separation Science and Technology, 43: 15, 3826 — 3841
To link to this Article: DOI: 10.1080/01496390802365787
URL: http://dx.doi.org/10.1080/01496390802365787

Separation Science and Technology, 15: 3826–3841, 2008

ISSN: 0149-6395 print/1520-5754 online
DOI: 10.1080/01496390802365787

Taylor & Francis
Taylor & Francis Group

Effects of Operating Modes on the Rejection Behavior using Ceramic Membranes

T. Y. Chiu,[1] F. J. Garcia-Garcia,[2] and A. E. James[3]
[1]School of Applied Sciences, Centre for Water Science,
Cranfield University, Bedfordshire, United Kingdom
[2]Corrosion and Protection Centre, School of Materials,
The University of Manchester, Manchester, United Kingdom
[3]School of Chemical Engineering and Analytical Science,
The University of Manchester, Manchester, United Kingdom

Abstract: Fouling generally occurs above the so-called "critical flux," below which steady-state membrane permeability is assumed to be attainable. Operation at sub-critical fluxes can thus be used to minimize membrane fouling. However, rejection behavior may be affected as a consequence of operating within this sub-critical mode that sustains the desirable permeate flux. In this study, the effluent from a synthetic activated sludge production process was used in the assessment of the performance of membrane microfiltration, as a pretreatment in desalination for wastewater reuse. The critical flux was identified using the step-by-step technique. Different operating regimes i.e. above and below the critical flux were used to assess the relationship between solute rejection and membrane fouling. When operating at sub critical mode, rejection was constant even under increasing transmembrane pressure (TMP). This arises mainly from the back transport of particles in the absence of cake formation. Beyond the critical regime, cake formation occurred and rejection increased with increasing TMP. At the critical regime, a decline in rejection was obtained. This rejection behavior was consistent over the three pore sizes that were investigated. Increasing the pore size appears to decrease the rejection at both regimes. This is because larger pore size allows the transmission of smaller particles and a less compact cake formation under and above the critical flux regime respectively. It appears from this study that one may be able to use rejection behavior to confirm and determine the

Received 22 April 2008; accepted 10 June 2008.
Address correspondence to T. Y. Chiu, School of Applied Sciences, Center for Water Science, Cranfield University, Bedfordshire, MK43 0AL, United Kingdom. Tel.: +44 01234 75 2835. Fax: +44 01234 75 1671. E-mail: t.chiu@cranfield.ac.uk

critical flux and adds to the confidence of using the step-by-step method to determine the critical flux.

Keywords: Critical flux, membrane performance, microfiltration, organic feed, rejection

INTRODUCTION

Membrane microfiltration is widely used in various wastewater treatment applications encompassing sewage effluent disinfection, decontamination of industrial effluents containing organic/inorganic pollutants, and as a pretreatment prior to reverse osmosis (RO) in wastewater reuse (1,2). Between using conventional biological treatment processes and membrane technology, the latter is the favored pre-treatment operation for RO due to their abilities to

1. produce high product water quality (free of bacteria and substantially reduced virus content)
2. reduce the chemicals use and
3. small footprint requirement (3).

Most importantly, the absolute retention of all microorganisms and particles (larger than the membrane's pore size) by a membrane significantly reduces the RO fouling susceptibility with suspended solids (SS), colloidal material, organics, bacteria, or scale from dissolved ions in the raw water. Earlier studies show that microfiltration pretreatment are more cost effective than conventional treatment methods and it enhances the RO permeate flux (4,5).

However, membrane fouling is still considered the "Achilles' heel'" of membranes technology and presents a major obstacle for efficient membrane operation. Fouling results in several deleterious effects including an increase in applied pressure required for a constant rate of water production, a decrease in water production due to declining permeate flux making frequent membrane replacement and cleaning necessary, a gradual membrane degradation which results in a shorter membrane life, and a decrease in permeate quality. A direct consequence of these is the increase in maintenance and operating costs. Reducing fouling is thus becoming a key issue in optimizing the separation process and can be achieved by operating microfiltration below the critical flux also known as the non-fouling regime. The concept of critical flux, J_{crit}, is defined as the balance between the forces linked to filtration pressure which maintains composites in the region of the membrane and shearing forces

which conversely hold them at a distance from it (6). The characteristic of operating in the sub critical regime is the absence of cake layer formation on the membrane surface. However, this property may affect the membrane surface characteristics such as rejection. Rejection depends on many parameters including the cake layer which is formed on the membrane surface or in the membrane matrix. Through fouling, the membrane properties i.e. the effective pore size distribution, through the blockage or partial blockage of the pores are modified and an added resistance to solute permeation by the cake layer on the membrane surface.

Most of the rejection studies undertaken relate to fouling with little information available on the impact of working below and above the critical flux regime on solute rejection. To this end, this work sets out to study the effect of operating regimes i.e. above J_{crit} and under J_{crit} on rejection using membranes of various pore sizes. The absence of fouling and the effect of this phenomenon, together with other characteristics such as back diffusion, are combined to explain the results.

EXPERIMENTAL

Membrane Feed

The membrane feed was the effluent of a synthetic activated sludge production system that uses the "Porous Pot" method as proposed by the Organization for Economic Coordination and Development (OECD) guidelines 302A and 303A (7), having a composition as shown in Table 1 following Nyholm et al. (8). These authors note that this composition of

Table 1. Composition of synthetic wastewater feed to the poros pot

Substance	Amount/ ($g\ l^{-1}$)	Molar concentration/ (10^{-3} M)
Meat Extract (International Diagnostics Group plc, UK)	11.0	0.6
Urea (Sigma Aldrich, UK)	3.0	47.9
Peptone(International Diagnostics Group plc, UK)	16.0	1.4
$CaCl_2 \cdot 2H_2O$ (BDH Chemicals Ltd, UK)	0.4	2.7
$Mg_2\ SO_4 \cdot 7H_2O$ (Fisons Scientific, UK)	0.2	0.7
K_2HPO_4 (Sigma Aldrich, UK)	2.8	16.1
NaCl (Sigma Aldrich, UK)	0.7	12.0

Table 2. Characteristics of membrane feed of the present study

pH	7.5
Total COD/(mg l^{-1})	67.7
SS content/(mg l^{-1})	313.1
TDS content/(mg l^{-1})	580.4
TS content/(mg l^{-1})	893.5
Zeta potential of particles/(mV)	−10.9

synthetic sewage medium achieved realistic sludge loading whilst the increased concentration of a phosphate buffer aid in avoiding pH drift.

Using the effluent from a well defined and stable synthetic sludge ensures that the experiments are reproducible and allowed work with a suspension that closely resembles effluent from an activated sludge based wastewater treatment plant (9). The present effluent was obtained from a stable bioreactor that had been running continually for more than 250 days (10). Although the pH of the effluent during the experimental period fluctuated slightly from pH 8.4 to pH 7.0, the results reported in this study are those obtained when the natural pH was at pH 7.5. No pH adjustments were carried out. The temperature of the sludge and suspensions were kept within the recommended range (7) of 20–25°C using a water bath thermostat.

The suspensions were characterized in terms of the chemical oxygen demand (COD), suspended solids (SS), total suspended solids (TSS), and total dissolved solids (TDS). COD was analyzed in accordance with method 508 C of standard methods (10). The particle size of the suspension was quantified with a laboratory particle size analyser (HYDRO 2000SM, Malvern Instruments, UK) which gives a distribution in terms of particle numbers. TSS and SS were determined in accordance with method 209 of standard methods (11). Table 2 presents the main biological characteristics of the effluent used as feed for membrane filtration for this study.

Membrane Filtration Unit

Ceramic membranes (Fairey Industrial Ceramics Ltd, England) with nominal pore diameter of 0.2, 0.35, 0.5 μm and seven star shaped flow channels used in this work were characterized and the results were detailed in previous work (12). The membrane and support were reported to be made of alumina and thicknesses of 60 and 8000 μm (obtained from SEM micrographs of fractured surfaces) respectively. These membranes

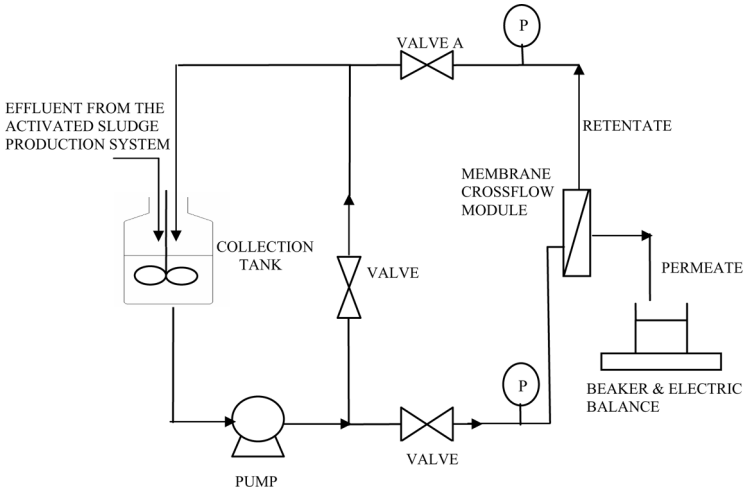

Figure 1. Schematic flow diagram of embrane filtration process.

having a filtration area of $0.03\,m^2$ and an equivalent hydraulic diameter of 2.3 mm were vertically mounted in a crossflow filtration module. Further details on the dimensions of the star shaped channels can be found in previous studies (13). A schematic diagram of the membrane filtration system used in the present study is shown in Fig. 1.

A crossflow velocity of $1.6\,ms^{-1}$ corresponding to the Reynolds number of 3700 was employed and achieved by using a recirculation peristaltic pump (Watson Marlow 603 S, UK). The Reynolds number was calculated using its equivalent hydraulic diameter. A previous study indicated that it was necessary for the filtration process to operate in the turbulent regime in order to optimize the flux performance of these membranes (14). The transmembrane pressure (TMP) was monitored using two pressure gauges (RS Components, UK) at either ends of the membrane module and controlled by closing the valve A to generate the backpressure.

Experimental Procedure

The step by step technique (14) was used to determine J_{crit} in this study. The transmembrane pressure was increased stepwise at fixed time intervals of 30 minutes prior to the onset of non-linearity in the increase in permeate flux, which was indicative of J_{crit}, thereafter 15 minutes time steps were used. The critical flux is the average between the last time independent flux step and the first time dependent step (see Fig. 2).

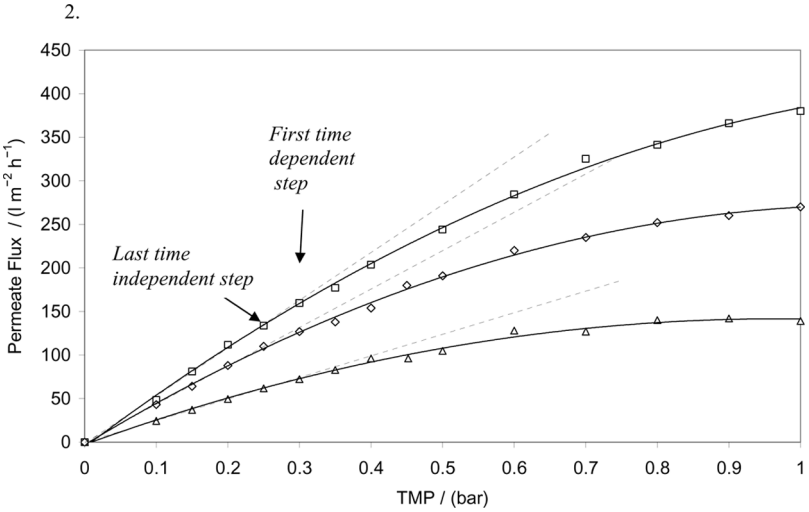

Figure 2. Determination of J_{crit} and ΔP_{crit} and at different pore sizes at pH 7.5 and cross flow velocity of 1.6 m s^{-1}, Δ: 0.2 μm, ◇: 0.35 μm □: 0.5 μm.

The pressure corresponding to the identified J_{crit} in the plot of permeate flux as a function of transmembrane pressure (TMP) is termed as the critical pressure, ΔP_{crit}. A maximum TMP of 1.0 bars was used in the determination of the critical fluxes.

Following J_{crit} and ΔP_{crit} determination, steady state crossflow filtrations were carried out over a range of TMP i.e. from the TMP below the ΔP_{crit} to that above the ΔP_{crit}. Additional analyses on the membranes after the filtration experiments employing $TMP > \Delta P_{crit}$ were carried out using scanning electron microscopy, SEM (FEI QUANTA 200, Purge, Czech Republic) to understand the nature of the process of cake formation.

After each run, the system was cleaned by circulating (highest setting of the motor) 0.1% w/v NaOH solution and 0.1% v/v nitric acid solution (BDH Chemicals Ltd, UK) at 40°C for 2 hours per solution. The rig was then rinsed with distilled water until the pH returned to 7. In order to ensure that the experiments had good reproducibility, the permeate flux was measured using distilled water after every cleaning operation. In the course of the study, changes in the distilled water flux through cleaned membranes were insignificant (<1%). Each J_{crit} and filtration measurement was repeated several times and the average value is reported here. All measurements show good reproducibility as the errors never exceed 5% in critical flux, steady state filtration and rejection characteristics.

RESULTS AND DISCUSSION

Critical Flux Evaluation

Figure 2 shows the permeate flux as a function of transmembrane pressure at a flow velocity of 1.6 m s^{-1}. The weak form of J_{crit} is observed for all the three pore sizes as the slopes of the linear relationships differ from that of the pure-water fluxes. Note that the straight lines in Fig. 2 are not pure water fluxes of the membranes but just the tangents drawn to illustrate the method of critical flux determination. The pure water fluxes through the 0.2, 0.35, and 0.5 μm membranes were approximately 80, 100, and 170 l $m^{-2}h^{-1}$ respectively at the TMP of 0.2 bars and cross-flow velocity of 1.6 ms^{-1}. This weak J_{crit} observation is in agreement with several workers (15,16) who attribute the weak form to adsorption and internal fouling changing the apparent membrane resistance. This characteristic is prevalent in most raw waters and also in secondary treated wastewater in which colloids and soluble organic are ubiquitous making clean water fluxes rarely attainable. The critical flux in this study is thus defined as the flux which characterized operation without formation of deposit on the membrane and if the TMP were increased above this critical value, the conventional behavior corresponding to the fouling phenomena and/or particle deposit will be observed up to the point where a plateau was reached as the filtration performance becomes substantially restricted (16). The critical pressure is identified to be 0.28 bars for all three pores. Although this method of determining J_{crit} has been reported to be subjective (17), the rejection behavior results shown and discussed later seem to support the obtained J_{crit}. Furthermore, care was taken to ensure that the step sizes used in this study was small enough for an accurate determination.

Effect of Flow Regime on Rejection

The retention was calculated by comparing the concentration of the substance in the permeate and that in the concentrate as follows:

$$R = \left[1 - \frac{C_p}{C_f}\right] \tag{1}$$

where R, C_p, and C_f are the retention, concentration in permeate and the concentration in feed respectively.

Figure 3 shows the rejection behavior of three pore size membranes as a function of the transmembrane pressure. At $\Delta P_{crit} < 0.28$ bars, a

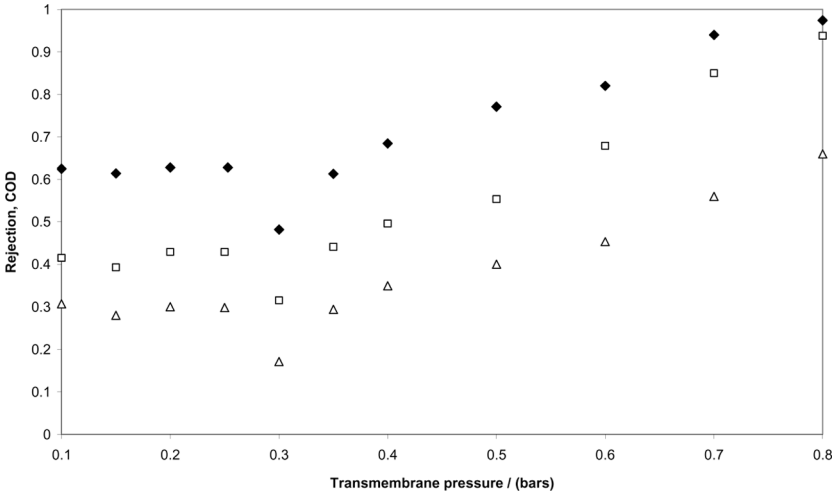

Figure 3. COD rejection at TMPs above and below ΔP_{crit} of 0.28 bars at different pore sizes at pH 7.5 and cross flow velocity of 1.6 m s^{-1}, ◆: 0.2 μm, □: 0.35 μm, Δ: 0.5 μm.

constant rejection was observed. Subsequently, when $\Delta P_{crit} = 0.28$ bars, rejection declines to a minimum and as $\Delta P_{crit} > 0.28$ bars, rejection increased with increasing TMP.

When operating steady state filtration at TMP $< \Delta P_{crit}$, filtration is thought to be operating under the non-fouling regime. The observed retention at this transient filtration stage is directly linked to the back transport of particles through diffusivity and lateral migration; in this case the particles remained in the retentate. Although increasing TMP within this regime would cause increased force on the particles towards the membrane, the rejection results seem to suggest that this force is insufficient to result in deposition which would inevitably change the retention characteristic of the surface. The observed retention is constant suggesting no additional resistance to the membrane permeation flux through surface modifications i.e. fouling. This implies that the rejection at this point is mainly due to the sieving mechanism of the membrane. An additional contributing factor to non-fouling arises from the electrical repulsions between the membrane and the particles. The isoelectric point of these membranes was reported to be pH 5.6 (12) and therefore under the current operating pH, the membrane would be negatively charged so is that of the suspension (Table 2). The repulsion prevents particles from depositing on the membrane.

When steady state filtration was carried out around the transition between the fouling and the non-fouling regime, a minimum rejection was observed and has been observed elsewhere (18). The results suggest that the stagnant layer of the retained compounds enhances polarization of the transmitted compounds despite the increase in filtration resistance. This falls within the first situation reported by van Oers et al. (19) who state that when the membrane rejects solutes better than the deposited layer, hindered back diffusion of solutes by the fouling layer results in solute accumulation near the membrane surface. This enhanced concentration polarization results in a steeper concentration gradient across the membrane and, hence, a decrease in solute rejection. This seems plausible as a partially developed deposit layer at or around J_{crit} is expected to form since it demarcates the transition of the fouling and the non-fouling regions. Although this behavior is reported mostly in NF and RO membranes (20), and in some instances UF membranes (18,19), this is highly applicable since the initial adsorption and internal pore blocking occurred to the membranes, a trait of the weak form of J_{crit}, would cause the MF membranes to act as a UF membrane.

The rejection increases with increasing TMP when filtration was carried out above ΔP_{crit} i.e. the fouling regime. In this regime, an improvement in the COD rejection occurs, when operating above J_{crit} than below J_{crit}, and may arise from the fully developed cake deposition as opposed to that at J_{crit}. This behavior falls into the second case reviewed by van Oers et al. (19) who state that when the solutes are rejected better by the deposited layer than by the membrane, the fouling layer controls the solute rejection and consequently improves it. Further, when TMP is increased, COD rejection increases. This implies that the increase in pressure differential reduces the COD transmission through an increase in the resistance of the fouling layer to permeation. This increase in resistance is likely to be due to an increase in fouling layer thickness coupled with a decrease in fouling layer voidage, both of which are expected to occur as a result of increasing the transmembrane pressure. Under this operation, it seems that hydrodynamics might play a more significant role in fouling since electrostatic repulsion between the membrane and the particles would still exist.

The explanations for the observed rejection trends are further supported by turbidity results (not shown here). Permeate turbidity has been often used as a measure of the quantity of macroscopical and the colloidal matter retained within the system. At $\Delta P_{crit} < 0.28$ bars, the permeate turbidity drops from 5.9 NTU to an almost constant 4.9 NTU. A further reduction of 0.8 NTU in the permeate turbidity was obtained at $\Delta P_{crit} > 0.28$ bars. This is suggestive that the initial constant turbidity was brought about through the sieving mechanism of the membrane

and as fouling occurs, additional rejection of colloidal matter by the cake on the membrane surface led to the increased clarity of the permeate. At $\Delta P_{crit} = 0.28$ bars, turbidity rose to 5.3 NTU. This suggests that an increased transmission of colloidal matters leading to a higher presence in the permeate and is in agreement with the explanation given above.

Effect of Pore Size on Rejection

Although the three pore size membranes show the same rejection trend, the level of retention seems to be dependant on the pore size (Fig. 3). Operating at subcritical fluxes, the idea that sieving mechanism of the pores through size exclusion being the main factor of the rejection behavior is reinforced as the rejection differences did not change significantly for all the pore sizes. An increase in the pore size led to a decrease in COD removal. This implies that the smaller pores allow for a lower transmission of chemically oxidizing compounds with the highest transmission occurring through the 0.5 μm pore sized membranes. This probably explains the increase in critical flux with pore sizes as shown in Fig. 2.

Above J_{crit}, higher rejection coefficients of both 0.2 and 0.35 μm are achieved compared to 0.5 μm. This observation is in agreement with that of other workers (21) and seems to suggest the presence of different resistances to permeate flow. It is known that fouling depends on the pore size and that fouling mechanisms occurring in larger pores are different from those occurring in smaller pores which would in turn affect the rejection behavior (22). Schäfer et al. (23) investigated the fouling effects on rejection for membranes on the microfiltration to nanofiltration scale and report an increase in rejection with fouling as a function of the pore size. In the present study, the SEM photographs of the fouled membranes seem to suggest that the main mechanisms for fouling are the same for each of the three pore-sizes i.e. both internal and external blocking (Fig. 4).

A plausible reason for this behavior is that the minimum particle size in the bimodal distribution of the feed is smaller than the three nominal pore sizes of the membranes employed (Fig. 5). This bimodal distribution is typically associated with wastewater containing bacteria and other microorganisms and is attributed to cell growth and the production of by–products arising from substrate metabolism and biomass decay during the complete mineralization of simple substrates (24). However, the extent of the internal blockage can be assumed to be different for each pore size. The smallest pore size of 0.2 μm may experience complete pore blockage compared to partial blockage in the largest pore size since the size of the smaller peak in the particle size distribution corresponds to

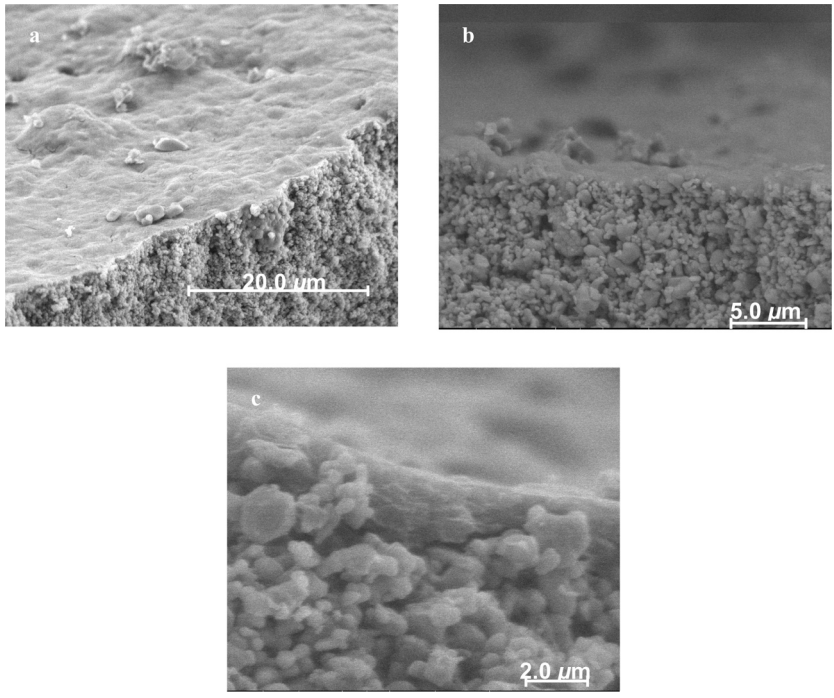

Figure 4. SEM micrograph of fouled membranes of different pore sizes from the side view. (a) 0.2 μm fouled membrane; (b) 0.35 μm fouled membrane; (c) 0.5 μm fouled membrane.

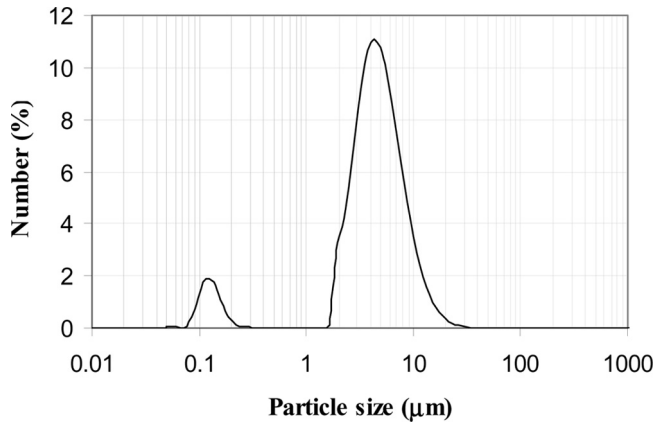

Figure 5. Particle size distribution of effluent from the Porous Pot system.

0.12 μm which is similar to the smallest pore size. The different reductions in pore size arising from internal blocking are reflected in the rejection behavior (Fig. 3) since smaller pores may experience a greater retention of particles.

Another contribution to the differences in the rejection behavior may arise from the difference in resistance which in turns arises from the differences in the cake structures for the three pores (Fig. 6). Figure 6 shows the formation of a more porous cake at larger pore sizes. In contrast, the foulant layer for the smallest pore seems to be very compact with little porosity. From the selective particle deposition point of view (25), the critical cut diameter of the deposited particles in the cross-flow filtration depends on the filtrate flux under the same cross-flow velocity. Larger pores result in a larger initial flux which encourages larger particles to be deposited (Fig. 5).

In addition, specific cake resistance calculations show increasing resistances with decreasing pore size (Table 3) with the smallest pore

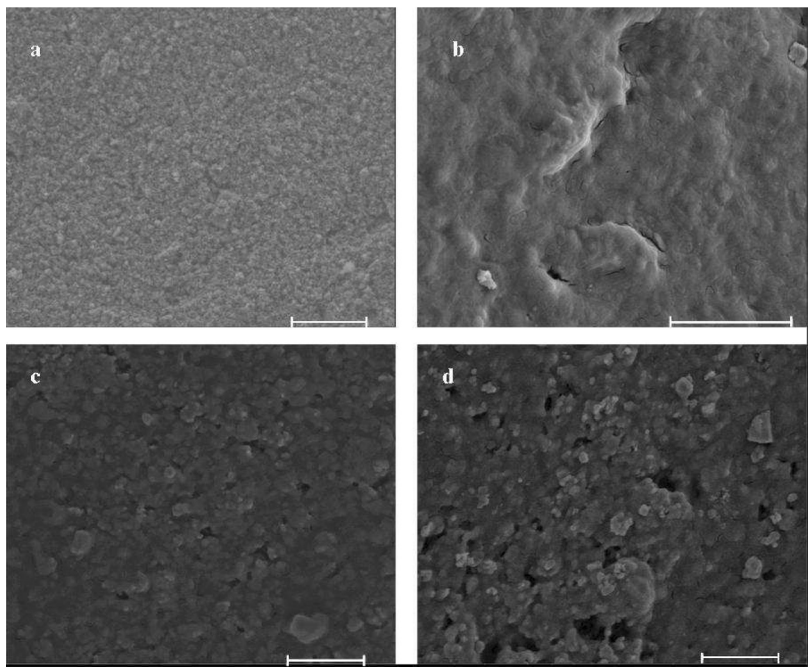

Figure 6. SEM micrographs of clean and fouled membranes of different pore sizes using 10 μm scale from the top view. (a) 0.2 μm clean membrane, (b) 0.2 μm fouled membrane, (c) 0.35 μm fouled membrane, (d) 0.5 μm fouled membrane.

Table 3. Specific cake resistance calculations from the flux time data

Pore size/(μm)	Specific cake resistance/(m^{-1})
0.2	10×10^6
0.35	8.0×10^6
0.5	4.0×10^6

producing the highest rejection over the range of TMP studied. This supports the surface observations (Fig. 6) that larger pores result in the formation of a larger porosity cake. These are in agreement with other workers (26) who attribute the increasing cake resistance to the retention of finer particles by membranes having smaller pores. The difference in cake resistance is known to be directly linked to the differences in rejection (27,28). This higher cake resistance seems to be associated with greater rejection as observed in the current work.

Another possibility, which is an extension of the above argument, is that all pores are not the nominal size and that there is a distribution of pore sizes. This is especially true in most commercial ceramic microfiltration membranes which could have a wider distribution than the particles (29–31). In addition to this, pores do not necessarily have a uniform diameter axially. An analogous effect to that occurring in deep bed filtration may result from the pore size distribution and narrowing in larger pores (32,33). This would allow material to build up in wide pores that are not continuous at the large diameter. Thus it is only when some fouling has occurred blocking these larger pores that the membranes, having a wider initial pore size, achieve the observed rejection as shown in Table 4.

Although this mechanism could explain the paradox of efficient rejection when large pores are present (see Table 4 for rejection data

Table 4. Solid retention in terms SS, TS, and TDS at cross-flow velocity = 1.6 m s^{-1}; pH 7.5; $\Delta P = 0.8$ bars for steady state filtration

	Permeate, C_p (rejection coefficient, R)		
Pore size (μm)	0.2	0.35	0.5
SS (mg l^{-1})	0.9 (1.0)	1.6 (0.99)	26.8 (0.91)
TS (mg l^{-1})	13.4 (0.99)	38.4 (0.96)	83.5 (0.91)
TDS (mg l^{-1})	12.5 (0.98)	36.8 (0.94)	56.7 (0.90)

for 0.5 μm pores) it only occurs when the pores are tapered. However, in order to validate this fouling mechanism, fully characterized model suspensions of known particle size would have to be used.

CONCLUSIONS

The effects of operating under different regimes i.e. above and below the critical flux on the rejection behavior of ceramic membranes of different pore sizes using a secondary effluent as a possible pretreatment step for reverse osmosis are evaluated. Rejection characteristics are shown to be dependant on hydrodynamics and membrane characteristics. Effluent microfiltration carried out under the different regimes led to three rejection characteristics. Below the critical regime, constant rejection is obtained. This is attributed to the natural sieving mechanism of the membranes. At the critical flux, a sudden increment of transmission is observed and may be the result of an enhanced polarisation effect. Above the critical flux, transmission decreased as TMP increased and is due to the formation of a cake layer which acts as an additional barrier. Rejection analysis of the transient filtration stage within the subcritical mode shows a higher initial transmission in larger pores which accounts for the higher critical flux achieved. Rejection performance of the membranes, in terms of COD removal, SS, and TDS, were better at smaller pore sizes. Different fouling mechanisms together with different cake structures could change the pore size distribution and could account for the observed differences in rejection. Finally, it appears from this study that one may be able to use rejection behavior to confirm and determine the critical flux and adds to the confidence of using the step-by-step method in determining J_{crit}.

ACKNOWLEDGEMENT

The authors are grateful to Universities UK for an Overseas Research Sponsorship award and to Fairey Ceramics Ltd, England for the supply of the membranes.

REFERENCES

1. AlMalack, M.H.; Anderson, G.K. (1997) Use of microfiltration in wastewater treatment. *Water Research*, *31*: 3064–3072.
2. Jacangelo, J.G.; Trussell, R.R.; Watson, M. (1997) Role of membrane technology in drinking water treatment in the United States. *Desalination*, *113*: 119–127.

3. Reith, C.; Bikehead, B. (1998) Membranes enabling the affordable and cost effective reuse of wastewater as an alternative source. *Desalination*, *117*: 203–210.
4. Adham, S.; Trussell, R.; Gagliardo, P.; Weibberg, K.; Richardson, T. (1997) Development of an innovative advanced treatment system for indirect potable reuse. Proceedings of the IDA World Congress on Desalination and Water Reuse, Madrid, Spain, Vol. II: 503–507.
5. Conklin, R.; Dunivin, W.R.; Herberg, J.D.; Leslie, G.L. (1996) *Advanced treatment using microfiltration and reverse osmosis reclaim secondary effluent in Orange County California*, Proceedings of the 16th Federal Convention Australian Water and Wastewater Association, Sydney, Australia.
6. Field, R.W.; Wu, D.; Howell, J.A.; Gupta, B.B. (1995) Critical flux concept for microfiltration fouling. *Journal of Membrane Science*, *100*: 259–272.
7. OECD, OECD Guidelines for Testing Chemicals, Organization for Economic Cooperation and Development. (1993) Paris, Guideline 302A & 303A.
8. Nyholm, N.; Berg, U.; Ingerslev, F. (1996) *Environmental Project No. 337—Activated Sludge Biodegradability Simulation Test*. Environmental Project 337, Miljøstyrelsen, Copenhagen, Denmark.
9. Christofi, N.; Aspichueta, E.; Dalzell, D.; De la Sota, A.; Etxebarria, J.; Fernandes, T.; Gutierrez, M.; Morton, J.; Obst, U.; Schmellenkamp, P. (2003) Congruence in the performance of model nitrifying activated sludge plants located in Germany, Scotland and Spain. *Water Research*, *37*: 177–187.
10. Lara-Dominguez, M.V.; James, A.E. (2005) *Analysis of sludge conditioning, Proceedings of the 7th World Congress of Chemical Engineering*, Glasgow, U.K.
11. APHA. (1992) Standard Methods for the Examination of Water and Wastewater, Section 5210, 18th ed. American Public Health Association Water Works Association, American Water Environment Federation, Washington, DC, 5.1–5.6.
12. Chiu, T.Y.; James, A.E. (2007) Electrokinetic characterisation techniques on asymmetric microfiltration membranes. *Colloids and Surfaces A: Physicochemical Engineering Aspects*, *301*: 281–288.
13. Chiu, T.Y.; James, A.E. (2006) Effects of axial baffles in non-circular multichannel ceramic membranes using organic feed. *Separation and Purification Technology*, *51*: 233–239.
14. Chiu, T.Y.; James, A.E. (2006) Critical flux enhancement in gas assisted microfiltration. *Journal of Membrane Science*, *281*: 274–280.
15. Gésan-Guiziou, G.; Boyaval, E.; Daufin, G. (1999) Critical stability conditions in crossflow microfiltration of skimmed milk: Transition to irreversible deposition. *Journal of Membrane Science*, *158*: 211–222.
16. Bouhabila, E.H.; Aim, R.B.; Buisson, H. (1998) Microfiltration of activated sludge using submerged membrane with air bubbling (application to wastewater treatment). *Desalination*, *118*: 315–322.
17. Bacchin, P.; Espinasse, B.; Aimar, P. (2005) Distributions of critical flux: Modelling, experimental analysis and consequences for cross-flow membrane filtration. *Journal of Membrane Science*, *250*: 223–234.

18. Chan, R.; Chen, V.; Bucknall, M.P. (2002) Ultrafiltration of protein mixtures: Measurement of apparent critical flux, rejection performance, and identification of protein deposition. *Desalination*, *146*: 83–90.
19. van Oers, C.W.; Vorstman, M.A.G.; Kerkhof, P.J.A.M. (1995) Solute rejection in the presence of a deposited layer during ultrafiltration. *Journal of Membrane Science*, *107*: 173–192.
20. Hoek, E.M.V.; Kim, A.S.; Elimelech, M. (2002) Influence of crossflow membrane filter geometry and shear rate on colloidal fouling in reverse osmosis and nanofiltration separations. *Environmental Engineering Science*, *19*: 357–372.
21. Gan, Q.; Allen, S.J. (1999) Crossflow microfiltration of a primary sewage effluent-solids retention efficiency and flux enhancement. *Journal of Chemical Technology and Biotechnology*, *74*: 693–699.
22. Van der Bruggen, B.; Geens, J.; Vandecasteele, C. (2002) Fluxes and rejections for nanofiltration with solvent stable polymeric membranes in water, ethanol and *n*-hexane. *Chemical Engineering Science*, *57*: 2511–2518.
23. Schäfer, A.I.; Fane, A.G.; Waite, T.D. (2000) Fouling effects on rejection in the membrane filtration of natural waters. *Desalination*, *31*: 215–224.
24. Noguera, D.R.; Araki, N.; Rittmann, B.E. (1994) Soluble microbial products (SMP) in anaerobic chemostats. *Biotechnology and Bioengineering*, *44*: 1040–1047.
25. Lu, W.M.; Ju, S.C. (1989) Selective particle deposition in cross-flow filtration. *Separation Science Technology*, *24*: 517–540.
26. Zhao, Y.; Zhong, J.; Li, H.; Xu, N.; Shi, J. (2002) Fouling and regeneration of ceramic microfiltration membranes in processing acid wastewater containing fine TiO_2 particles. *Journal of Membrane Science*, *208*: 331–341.
27. Chang, I.S.; Bag, S.O.; Lee, C.H. (2001) Effects of membrane fouling on solute rejection during membrane filtration of activated sludge. *Process Biochemistry*, *36*: 855–860.
28. Yildiz, E.; Nuhoglu, A.; Keskinler, B.; Akay, G.; Farizoglu, B. (2003) Water softening in a crossflow membrane reactor. *Desalination*, *159*: 139–152.
29. Marshall, A.D.; Munro, P.A.; Tragardh, G. (1993) The effect of protein fouling in microfiltration and ultrafiltration on permeate flux, protein retention and selectivity: A literature review. *Desalination*, *91*: 65–108.
30. Persson, K.M.; Capannelli, G.; Bottino, A.; Trägårdh, G. (1993) Porosity and protein adsorption of four polymeric microfiltration membranes. *Journal of Membrane Science*, *76*: 61–71.
31. Chowdhury, S.R.; Schmuhl, R.; Keizer, K.; ten Elshof, J.E.; Blank, D.H.A. (2003) Pore size and surface chemistry effects on the transport of hydrophobic and hydrophilic solvents through mesoporous γ-alumina and silica MCM-48. *Journal of Membrane Science*, *225*: 177.
32. Holdich, R.G.; Cumming, I.W.; Kosvintsev, S.; Bromley, A.J.; Stefanini, G. (2003) Clarification by slotted surface microfilters. *Minerals Engineering*, *16*: 121–128.
33. Rushton, A.; Ward, A.S.; Holdich, R.G. (2000) Solid–Liquid Filtration and Separation Technology, VCH-Wiley, Weinheim, Germany.